JACS
JOURNAL OF THE AMERICAN CHEMICAL SOCIETY

Communication

Nanoparticles with Near-Infrared Emission Enhanced by Pillararene-Based Molecular Recognition in Water

Bingbing Shi, Kecheng Jie, Yujuan Zhou, Jiong Zhou, Danyu Xia, and Feihe Huang

J. Am. Chem. Soc., **Just Accepted Manuscript** • DOI: 10.1021/jacs.5b11676 • Publication Date (Web): 23 Dec 2015

Just Accepted

ACS Publications

Journal of the American Chemical Society is published by the American Chemical Society. 1155 Sixteenth Street N.W., Washington, DC 20036

Nanoparticles with Near-Infrared Emission Enhanced by Pillararene-Based Molecular Recognition in Water

Bingbing Shi, Kecheng Jie, Yujuan Zhou, Jiong Zhou, Danyu Xia, and Feihe Huang*

State Key Laboratory of Chemical Engineering, Department of Chemistry, Zhejiang University, Hangzhou 310027, P. R. China

Fax and Tel: +86-571-8795-3189; Email: fhuang@zju.edu.cn

ABSTRACT: Here we report the unprecedented preparation of nanoparticles with near-infrared emission enhanced by host–guest complexation between a water-soluble pillar[5]arene (**WP5**) and a cyanostilbene derivative (**1**) in water. Amphiphilic **1** self-assembles in water to form nanoribbons with relatively weak near-infrared emission at low concentrations. However, after addition of equimolar **WP5**, these nanoribbons transform into nanoparticles with stronger near-infrared emission due to the formation of a supramolecular amphiphile and host–guest complexation induced aggregation. These nanoparticles show pH responsiveness, and collapse after treatment with acid. More importantly, these nanoparticles can be used in living cell imaging.

Fluorescent self-assembled materials with well-designed structures and morphologies have attracted great interest of scientists in recent years due to their applications in numerous fields including light–energy conversion, molecular electronics, catalysis, sensors, drug delivery, and cell imaging.[1] In particular, fluorescent organic nanomaterials, which have excellent flexibility for chemical modification, are beneficial for diagnosis, real-time cell imaging, and treatment of diseases.[2] Although a lot of very good fluorescent self-assembled materials with well-defined morphologies have been obtained by rational-designed small molecules, many of them can not be used for biomedical application due to their lack of near-infrared (NIR) emission (650–900 nm) and inherent fluorescence quenching.[3] It has been well-known that NIR fluorescent emission can realize very small photo-damage to biological samples, minimum interference from biomolecule autofluorescence, and deep tissue penetration.[4] Although great efforts have been made to the development of excellent "aggregation-induced emission" (AIE) and "aggregation-induced enhanced emission" (AIEE) fluorescent self-assembled materials since the first report of AIE active molecules by Tang and coworkers, the majority of AIE-active materials have the emission wavelengths below 650 nm.[5]

Pillar[*n*]arenes,[6] which are linked by methylene (-CH_2-) groups at the *para*-positions of 2,5-dialkoxybenzene rings, mainly include pillar[5]arenes[7] and pillar[6]arenes.[8] They are an emerging type of macrocyclic hosts after cyclodextrins,[9] calixarenes,[10] crown ethers,[11] cucurbiturils[12] and cavitands.[13] Pillararenes have a pillar architecture, in sharp contrast to the basket-shaped architecture of calixarenes. Their symmetrical structures and easy functionalization afford them with excellent properties in host–guest chemistry.[14] Based on the great efforts made by chemists and materials scientists, numerous stimuli-responsive host–guest recognition motifs of pillararenes have been built and further applied in the fabrication of various materials, including pillararene-based supramolecular polymers and supramolecular amphiphiles.[7,8,15] However, most of these studies have been focused on the responsivenesses of these supramolecular materials to external stimuli. In sharp contrast, only a few efforts have been made to explore fluorescent properties of pillararene-based host–guest systems and their ensembles.[16] More importantly, pillararene-based NIR fluorescent materials have not been reported. The lack of such materials may greatly impede the use of pillararenes in the field of fluorescent materials. Therefore, it is important and necessary to design and prepare NIR fluorescent supramolecular nanomaterials based on pillararene-based molecular recognition. Here we report the unprecedented preparation of nanoparticles with NIR emission induced by pillararene-based molecular recognition in water.

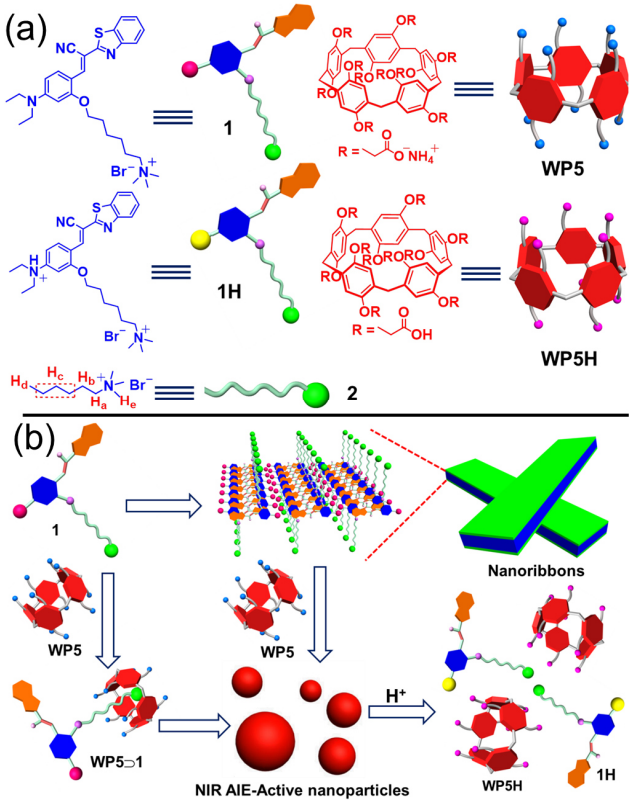

Scheme 1. (a) Chemical structures and cartoon representations of **1**, **1H**, **2**, **WP5**, and **WP5H**; (b) Cartoon representation of self-assemblies of **1** and **WP5⊃1** and pH responsiveness of nanoparticles prepared from **WP5⊃1**.

Our design of these nanoparticles is shown in Scheme 1. Different from the traditional AIE fluorescent molecules, which require excitation by cell–damaging ultraviolet irradiation, cyanostilbene derivatives absorb strongly in the visible region and emit brightly in the red to NIR range of the flourescent spectrum.[17] When they are triggered by aggregation or crystallization, the fluorescent emission intensity of the cyanostilbene derivatives greatly increases upon the formation of a dimer. Therefore, cyanostilbene derivatives are very good

building blocks for the fabrication of NIR AIE-active nanomaterials. In view of this, in order to introduce NIR emission, here cyanostilbene derivative **1** (Scheme 1) is used as a building block in the construction of our NIR emission nanoparticles. However, amphiphilic **1** self-assembles into nanoribbons with relatively weak emission in water driven by π-π stacking interactions between the cyanostilbene groups and hydrophobic interactions (Figure 1).[18] Interestingly, these nanoribbons transform into nanoparticles after addition of water-soluble pillar[5]arene **WP5** because of the formation of a supramolecular amphiphile **WP5⊃1** (Scheme 1 and Figure 1), and the resultant nanoparticles show much stronger NIR fluorescent emission due to the host–guest complexation induced aggregation, which is a result of the solubility decrease after complexation. These fluorescent nanoparticles are pH-responsive, and they collapse after treatment with acid. More importantly, they are red emitters in the aggregated state, and their fluorescent spectrum covers the NIR range, enabling them as imaging agents for living cells.

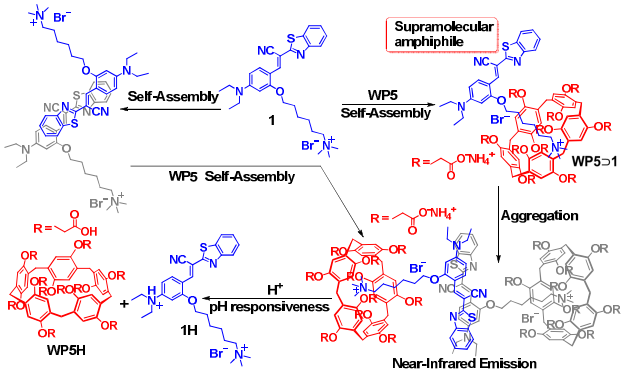

Figure 1. Mechanisms of the aggregation processes of **1** and **WP5⊃1** and pH responsiveness of **WP5⊃1** in water.

It has been well-established that pillararenes can complex with positively-charged guests.[8b] Because **1** contains a trimethylammonium group, we wondered whether **1** could complex with **WP5** to form a supramolecular amphiphile. In order to confirm this, we first studied the host–guest complexation between **WP5** and **1** by ^{1}H NMR. *N,N,N*-trimethylhexan-1-aminium bromide (**2**) was used as a model guest due to the relatively poor water-solubility of **1**. According to the proton NMR spectrum of an equimolar (10.0 mM) aqueous solution of **WP5** and **2**, the complexation rapidly exchanges on the proton NMR timescale (Figure S10). Peaks related to protons H_{a-e} on **2** shifted upfield after complexation. Meanwhile, peaks related to protons H_{1-3} on **WP5** shifted downfield. Furthermore, a 2D NOESY NMR study of the aqueous solution of **2** and **WP5** was performed to investigate the relative spatial positions of protons in this host–guest complex (Figure S11). Correlation signals were observed between protons H_{a-d} on **2** and protons H_{1-3} on **WP5**. These results indicated that the positively-charged trimethylammonium head of **2** was threaded into the cavity of the cyclic host **WP5** to form a pseudorotaxane.

In order to determine the association constant (K_a) of the host–guest complex between **WP5** and **2**, we carried out isothermal titration calorimetry (ITC) experiments to provide thermodynamic insight into the complex (Figure S12). The K_a value of **WP5⊃2** was determined to be $(1.75 \pm 0.21) \times 10^6$ M^{-1} in 1:1 complexation mode. The cooperativity of multiple electrostatic interactions between the carboxylate anionic groups on **WP5** and the cationic trimethylammonium group of **2**, and hydrophobic interactions in aqueous solution endow the high binding affinity of this host–guest complex.

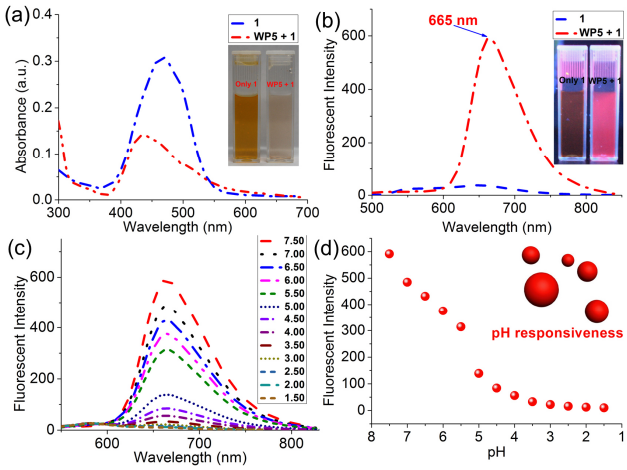

Figure 2. (a) Absorbance spectra of **1** (5.00×10^{-5} M) in aqueous PBS buffer solution (APBSBS) without and in the presence of **WP5**. Inset: photograph showing the color change from **1** to **WP5⊃1** in APBSBS. (b) Fluorescence spectral response of **1** (5.00×10^{-5} M) in APBSBS upon addition of 1.0 equiv. of **WP5** (λ_{ex} = 470 nm). Inset: photograph of **1** and **WP5⊃1** (5.00×10^{-5} M) under a UV-lamp (365 nm). (c) Influence of pH on the fluorescence of **WP5⊃1** in APBSBS (λ_{ex} = 470 nm). (d) Solution pH dependence of the fluorescence intensity of **WP5⊃1** in APBSBS at 665 nm.

After we established the **WP5⊃2** recognition motif, a supramolecular amphiphile by simply mixing **WP5** with **1** in water was prepared. Several experiments were performed to confirm the formation of this supramolecular amphiphile. The UV/Vis absorption and fluorescent emission measurements on **1** and **WP5⊃1** were firstly performed in aqueous PBS (phosphate buffer saline) buffer solution (1.00×10^{-2} M PBS, pH = 7.4). As shown in Figures 2a and 2b, the UV/Vis absorption and emission spectra of 5.00×10^{-5} M **1** in aqueous PBS buffer solution exhibited an absorption maximum at 470 nm and a weak emission band, respectively. Upon addition of equimolar **WP5**, a new emission band centered at 665 nm appeared in the fluorescent spectrum, directly leading to a much strong NIR emission. In the aqueous solution of **WP5⊃1**, the trimethylammonium group of **1** was threaded into the cavity of **WP5** and the aggregation was enhanced because **WP5⊃1** had lower water-solubility than **1**, resulting in an intense "turn-on" emission signal (Figure 1).[18] In order to further investigate the aggregation effect, concentration-dependent fluorescent spectra of **1** were utilized to study the aggregation ability of **1** and the weak fluorescent emission property of the nanoribbons self-assembled from **1**. As shown in Figure S13, **1** has very weak emission at low concentrations (< 1.00×10^{-4} M). With the increase of the concentration of **1** in aqueous PBS buffer solution, the fluorescence intensity of **1** was enhanced gradually due to the aggregation effect of **1** and the formation of nanoribbons. In addition, as shown in Figure S14, after addition of **WP5** to a solution of the nanoribbons, a higher emission band centered at 665 nm appeared in the fluorescence spectrum, directly leading to a much strong NIR emission due to the formation of nanoparticles. These observations indicated that both the nanoribbons and nanoparticles have fluorescent emission, but the nanoparticles show much stronger emission than the nanoribbons at the same concentrations of **1** and **WP5⊃1** at low concentrations, which is attributed to the host–guest complexation enhanced aggregation.

From our previous work,[19] we know that the complex **WP5⊃1** can be easily destroyed by acid, since acid protonates the carboxylate groups to convert **WP5** to **WP5H** (Scheme 1 and

Figure 1), resulting in **WP5H** precipitation from the aqueous solution. Meanwhile, the nitrogen atom of **1** on the diethylamine group can also be easily protonated by acid (Scheme 1 and Figure 1),[20] which converts **1** into water-soluble salt **1H** (Figure S19). Hence, the fluorescence of the **WP5⊃1** system is nearly quenched after addition of acid. Figures 2c and 2d show that the fluorescent intensity of the **WP5⊃1** system decreased rapidly after the addition of acid. When the pH of the aqueous PBS buffer solution (1.00×10^{-2} M PBS) of **WP5** (5.00×10^{-5} M) and **1** (5.00×10^{-5} M) is 4.00, the fluorescent emission is nearly quenched.

The investigation of the self-assembly behaviour of **1** and **WP5⊃1** also confirmed the formation of the supramolecular amphiphile. When **1** was dissolved in water, the conductivity of the solution as a function of the concentration of **1** was measured to determine its critical aggregation concentration (CAC).[21] The two linear segments in the curve and a sudden reduction of the slope indicate that the CAC value of **1** is approximately 1.00×10^{-4} M (Figure S17). The self-assembly behaviour of **1** was subsequently investigated in water by scanning electron microscopy (SEM) and transmission electron microscopy (TEM). SEM and TEM experiments helped in the visualization of the self-assembled nanostructures from **1**. Figure 3a shows an SEM micrograph of **1** aggregates. Ribbon-like aggregates about 20 μm in length and 100 nm in width were obtained. A TEM experiment also revealed the ribbon-like assemblies (Figure 3b).

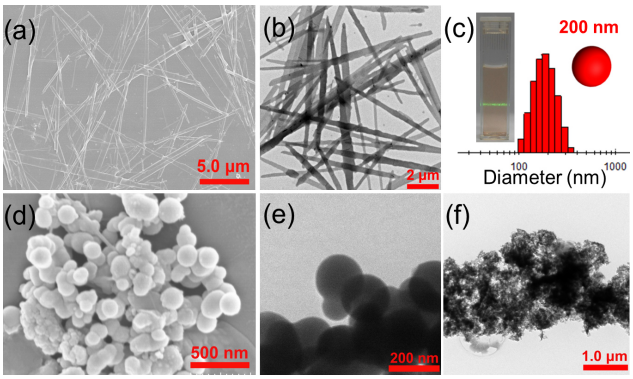

Figure 3. (a) SEM image of the nanoribbon aggregates of **1** (1.00×10^{-3} M); (b) TEM image of the nanoribbon aggregates of **1** (1.00×10^{-3} M); (c) DLS study and Tyndall effect of the host–guest complex **WP5⊃1** assemblies (1.00×10^{-3} M); (d) SEM image of the nanoparticles of **WP5⊃1** (1.00×10^{-3} M); (e) TEM image of the nanoparticles of **WP5⊃1** (1.00×10^{-3} M); (f) TEM image of **WP5⊃1** complex after the addition of H^+ in pure water (1.00×10^{-3} M).

However, the CAC value of **WP5⊃1** in pure water was measured to be ~5.00×10^{-5} M (Figure S18), lower than that of **1**. A Tyndall effect (Figure 3c) was observed for a solution of **WP5⊃1**, indicating the average diameter of the self-assemblies was >100 nm. DLS results (Figures 3c and S20) showed that the aggregates of **WP5⊃1** have an average diameter of ~200 nm with a narrow size distribution at different concentrations. Furthermore, spherical assemblies around 200 nm in diameter were observed by SEM (Figure 3d), supporting the DLS results. A TEM experiment was conducted and solid spherical assemblies were also observed, suggesting that **WP5⊃1** self-assembled into nanoparticles in water (Figure 3e). What's more, when the pH of the aqueous solution of **WP5** and **1** decreased to 4.00, the self-assembly morphology of **WP5⊃1** changed from nanoparticles to irregular aggregates since the complex **WP5⊃1** was destroyed (Figure 3f). These results indicated that this supramolecular amphiphile had pH responsiveness.

With the NIR nanoparticles in hand, we wondered whether they could be applied in biological and pharmaceutical fields. Before doing so, we firstly evaluated the toxicity of **WP5**, **1**, and **WP5⊃1**. A 3-(4,5-dimethylthiazol-2-yl)-2,5-diphenyltetrazolium bromide (MTT) assay was carried out to evaluate the cytotoxicity for **WP5**, **1**, and **WP5⊃1** at different concentrations against human cervical carcinoma cell (HeLa) and brain microvasular endothelial cell (bEnd.3). As show in Figure S21, after incubated with **WP5** for 4 h with the concentration ranging from 20 to 160 μg/mL, HeLa and bEnd.3 cells show the minimal influence on cell viability and proliferation, indicating that **WP5** has good biocompatibility and low toxicity. On the other hand, **1** showed relatively high toxicity against HeLa and bEnd.3 cells. A decrease in relative cell viability was detected with the increase of the concentration of **1**. In contrast, the relative cell viability of **1** was lower than that of the host–guest complex **WP5⊃1** at the same concentration, which indicated that the formation of the host–guest complex reduced the toxicity of **1**.

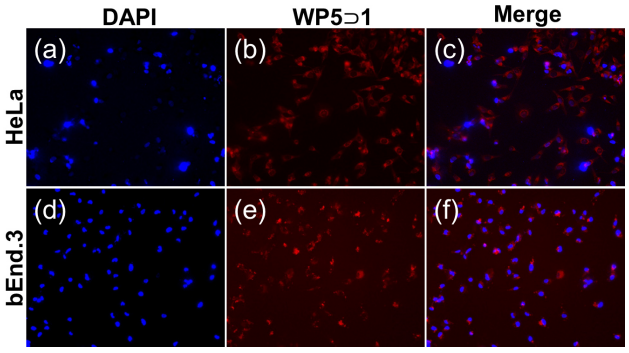

Figure 4. Confocal images of live HeLa and bEnd.3 cells after incubation with **WP5⊃1** (**WP5⊃1** concentration is 5.00×10^{-4} M) for 4 h: (a) and (d) stained with DAPI; (b) and (e) fluorescent image; (c) merged image from (a) and (b); (f) merged image from (d) and (e).

Furthermore, the nanoparticles self-assembled from **WP5⊃1** were utilized as a living cell imaging agent. HeLa and bEnd.3 cells were treated with **WP5⊃1** for 4 h. We then used confocal laser scanning microscopy to monitor the intracellular distribution of the **WP5⊃1** assemblies. Both HeLa and bEnd.3 cells treated with **WP5⊃1** exhibited bright red fluorescent emission in the cytoplasm of the cells (Figures 4, S22 and S23). These observations indicated that the **WP5⊃1** assemblies can be successfully applied for living cells imaging.

In summary, novel NIR AIE-active nanoparticles were fabricated by employing the host–guest complex **WP5⊃1** as a building block. In contrast to the nanoribbons self-assembled from **1**, supramolecular amphiphile **WP5⊃1** self-assembled into nanoparticles. The nanoribbons show relatively weak fluorescent emission, while the nanoparticles show very strong NIR fluorescent emission at the same concentrations of **1** and **WP5⊃1** at low concentrations because of the host–guest complexation enhanced aggregation. Furthermore, these nanoparticles were utilized as an imaging agent for living cells due to their NIR emission. This is the first time that NIR AIE-active nanoparticles were constructed by pillararene-based host–guest interactions and used for living cell imaging. Therefore, here we reported an unprecedented method for the preparation of NIR emissive nanoparticles based on pillararene host–guest chemistry. These results indicated that pillararene-based host–guest complexes have enormous potential in biological and pharmaceutical fields, including cell imaging, drug and gene delivery, and biosensors.

ASSOCIATED CONTENT

Supporting Information

Experimental details, NMR spectra, and other materials. These material are available free of charge via the Internet at http://pubs.acs.org.

AUTHOR INFORMATION

Corresponding Author

fhuang@zju.edu.cn

Notes

The authors declare no competing financial interest.

ACKNOWLEDGMENT

This work was supported by National Basic Research Program (2013CB834502), the National Natural Science Foundation of China (21125417, 21434005), the Fundamental Research Funds for the Central Universities, the Key Science Technology Innovation Team of Zhejiang Province (2013TD02), and Open Project of State Key Laboratory of Supramolecular Structure and Materials (sklssm201509).

REFERENCES

1 (a) Zhao, Y.; Fu, H.; Peng, A.; Ma, Y.; Liao, Q.; Yao, J. *Acc. Chem. Res.* **2010**, *43*, 409−418. (b) Zheng, H.; Li, Y.; Liu, H.; Yin, X.; Li, Y. *Chem. Soc. Rev.* **2011**, *40*, 4506−4524. (c) He, B.; Dai, J.; Zherebetskyy, D.; Chen, T. L.; Zhang, B. A.; Teat, S. J.; Zhang, Q.; Wang. L.; Liu, Y. *Chem. Sci.* **2015**, *6*, 3180–3186.

2 (a) Hu, X. L.; Hu, J. M.; Tian, J.; Ge, Z. S.; Zhang, G. Y.; Luo, K. F.; Liu, S. Y. *J. Am. Chem. Soc.* **2013**, *135*, 17617−17629. (b) Anees, P.; Sreejith, S.; Ajayaghosh, A. *J. Am. Chem. Soc.* **2014**, *136*, 13233–13239. (c) Lee, M. H.; Park, N.; Yi, C.; Han, J. H.; Hong, J. H.; Kim, K. P.; Kang, D. H.; Sessler, J. L.; Kang, C.; Kim, J. S. *J. Am. Chem. Soc.* **2014**, *136*, 14136–14142.

3 (a) Yuan, L.; Lin, W. Y.; Zheng, K. B.; He, L. W.; Huang, W. M. *Chem. Soc. Rev.* **2013**, *42,* 622–661. (b) Shao, A. D.; Xie, Y. S.; Zhu, S. J.; Guo, Z. Q.; Zhu, S. Q.; Guo, J.; Shi, P.; James, T. D.; Tian, H.; Zhu, W. H. *Angew. Chem. Int. Ed.* **2015**, *54*, 7275–7280.

4 (a) Weissleder, R.; Pittet, M. J. *Nature* **2008**, *452*, 580–589; (b) Liu, Y.; Chen, M.; Cao, T. Y.; Sun, Y.; Li, C. Y.; Liu, Q.; Yang, T. S.; Yao, L. M.; Feng, W.; Li, F. Y. *J. Am. Chem. Soc.* **2013**, *135*, 9869–9876.

5 (a) Zhu, L.; Li, X.; Zhang, Q.; Ma, X.; Li, M.; Zhang, H.; Luo, Z.; Ågren, H.; Zhao, Y. *J. Am. Chem. Soc.* **2013**, *135*, 5175–5182. (b) Kwok, R. T. K. C.; Leung, W.; Lam, J. W. Y.; Tang, B. Z. *Chem. Soc. Rev.* **2015**, *44*, 4228–4238.

6 (a) Kanai, S.; Nojiri, Y.; Konishi, G.; Nakamoto, Y. *Polym. Prep. Jpn. J.* **2006**, *55*, 303. (b) Ogoshi, T.; Kanai, S.; Fujinami, S.; Yamagishi, T.; Nakamoto, Y. *J. Am. Chem. Soc.* **2008**, *130*, 5022–5023. (c) Cao, D.; Kou, Y.; Liang, J.; Chen, Z.; Wang, L.; Meier, H. *Angew. Chem. Int. Ed.* **2009**, *48*, 9721–9723.

7 (a) Li, C.; Shu, X.; Li, J.; Chen, S.; Han, K.; Xu, M.; Hu, B.; Yu, Y.; Jia, X. *J. Org. Chem.* **2011**, *76*, 8458–8465. (b) Yao, Y.; Xue, M.; Chen, J.; Zhang, M.; Huang, F. *J. Am. Chem. Soc*. **2012**, *134*, 15712−15715. (c) Zhang, H.; Nguyen, K. T.; Ma, X.; Yan, H.; Guo, J.; Zhu, L.; Zhao, Y. *Org. Biomol. Chem.* **2013**, *11*, 2070–2074.

8 (a) Yu, G.; Zhou, X.; Zhang, Z.; Han, C.; Mao, Z.; Gao, C.; Huang, F. *J. Am. Chem. Soc*. **2012**, *134*, 19489–19497. (b) Xue, M.; Yang, Y.; Chi, X.; Zhang, Z.; Huang, F. *Acc. Chem. Res*. **2012**, *45*, 1294–1308.

9 (a) Harada, A.; Takashima, Y.; Yamaguchi, H. *Chem. Soc. Rev.* **2009**, *38*, 875–882. (b) Ma, X.; Tian, H. *Acc. Chem. Res*. **2014**, *77*, 1971–1981.

10 (a) Guo, D.-S.; Liu, Y. *Chem. Soc. Rev.* **2012**, *41*, 5907–5921. (b) Kim, S. K.; Lynch, V. M.; Sessler, J. L. *Org. Lett.* **2014**, *16*, 6128–6131.

11 (a) Jones, J. W.; Zakharov, L. N.; Rheingold, A. L.; Gibson, H. W. *J. Am. Chem. Soc.* **2002**, *124*, 13378–13379. (b) Jiang, W.; Schalley, C. A. *Proc. Natl. Acad. Sci. U.S.A.* **2009**, *106*, 10425–10429. (c) Zhu, K.; Vukotic, V. N.; Loeb, S. J. *Angew. Chem. Int. Ed.* **2012**, *51*, 2168–2172. (d) Lu, T.-W.; Chang, C.-F.; Lai, C.-C.; Chiu, S.-H. *Angew. Chem. Int. Ed.* **2013**, *52*, 10231–10236. (e) Tian, Y.-K.; Shi, Y.-G.; Yang, Z.-S.; Wang, F. *Angew. Chem. Int. Ed.* **2014**, *53*, 6090–6094.

12 (a) Kim, K. *Chem. Soc. Rev.* **2002**, *31*, 96−107. (b) Vinciguerra, B.; Cao, L.; Cannon, J. R.; Zavalij, P. Y.; Fenselau, C.; Isaacs, L. *J. Am. Chem. Soc.* **2012**, *134*, 13133. (c) Barrio, J.; Horton, P. N.; Lairez, D.; Lloyd, G. O.; Toprakcioglu, C.; Scherman, O. A. *J. Am. Chem. Soc.* **2013**, *135*, 11760−11763.

13 (a) Pinalli, R.; Cristini, V.; Sottili, V.; Geremia, S.; Campagnolo, M.; Caneschi, A.; Dalcanale, E. *J. Am. Chem. Soc.* **2004**, *126*, 6516−6517. (b) Hooley, R. J.; Rebek, J., Jr. *J. Am. Chem. Soc.* **2005**, *127*, 11904–11905. (c) Gan, H. Y.; Benjamin, C. J.; Gibb, B. C. *J. Am. Chem. Soc.* **2011**, *133*, 4770–4773.

14 (a) Strutt, N. L.; Forgan, R. S.; Spruell, J. M.; Botros, Y. Y.; Stoddart, J. F. *J. Am. Chem. Soc.* **2011**, *133*, 5668–5671. (b) Yu, G.; Han, C.; Zhang, Z.; Chen, J.; Yan, X.; Zheng, B.; Liu, S.; Huang, F. *J. Am. Chem. Soc.* **2012**, *134*, 8711–8717. (c) Li, H.; Chen, D.-X.; Su, Y.-L.; Zheng, Y.-B.; Tan, L.-L.; Weiss, P.-S.; Yang, Y.-W. *J. Am. Chem. Soc.* **2013**, *135*, 1570–1576.

15 (a) Zhang, Z.; Luo, Y.; Chen, J.; Dong, S.; Yu, Y.; Ma, Z.; Huang, F. *Angew. Chem. Int. Ed.* **2011**, *50*, 1397–1401. (b) Duan, Q.; Yu,; Yan, C. L.; Hu, X.; Xiao, T.; Lin, C.; Pan, Y.; Wang, L. *J. Am. Chem. Soc.* **2013**, *135*, 10542–10549. (c) Chang, Y.; Yang, K.; Wei, P.; Huang, S.; Pei, Y.; Zhao, W.; Pei, Z. *Angew. Chem. Int. Ed.* **2014**, *53*, 13126–13130.

16 (a) Maffei, F.; Betti, P.; Genovese, D.; Montalti, M.; Prodi, L.; Zorzi, R. D.; Geremia, S.; Dalcanale, E. *Angew. Chem. Int. Ed.* **2011**, *50*, 4654–4657. (b) Wu, J. S.; Kwon, B.; Liu, W. M.; Anslyn, E. V.; Wang, P. F.; Kim, J. S. *Chem. Rev.* **2015**, *115*, 7893−7943.

17 Han, G.; Kim, D.; Park, Y.; Bouffard, J.; Kim, Y. *Angew. Chem. Int. Ed.* **2015**, *54,* 3912–3916.

18 (a) Wang, M.; Zhang, D.; Zhang, G.; Tang, Y.; Wang, S.; Zhu, D. *Anal. Chem.* **2008**, *80*, 6443–6448. (b) Zhang, R.; Tang, D.; Lu, P.; Yang, X.; Liao, D.; Zhang, Y.; Zhang, M.; Yu, C.; Yam, V. W.-W. *Org. Lett.* **2009**, *11*, 4302–4305.

19 Yao, Y.; Chi, X.; Zhou, Y.; Huang, F. *Chem. Sci.* **2014**, *5*, 2778–2782.

20 (a) Yao, S.; Katherine, J.; Belfield, K. D. *Org. Lett.* **2007**, *9*, 5645–5648. (b) Kim, E. H.; Lee, S. H.; Park, S. B. *Chem. Commun.* **2011**, *47*, 7734–7736.

21 Sun, Y.; Yan, C.-G.; Yao, Y.; Han, Y.; Shen, M. *Adv. Funct. Mater.* **2008**, *18*, 3981–3990.

TOC Graphic: